Supplementary information

Directly measuring the structural transition pathways of strain-engineered VO_2 thin films

Egor Evlyukhin,[a]* Sebastian A. Howard,[a] Hanjong Paik,[b,c] Galo J. Paez,[a] David J. Gosztola,[d] Christopher N. Singh,[a] Darrell G. Schlom,[b,e] Wei-Cheng Lee[a] and Louis F. J. Piper[a]*

[a]*Department of Physics, Applied Physics and Astronomy, Binghamton University, Binghamton, New York 13902, USA*

[b]*Departments of Materials Science and Engineering, Cornell University, Ithaca, New York 14853-1501, USA*

[c]*Platform for the Accelerated Realization, Analysis and Discovery of Interface Materials (PARADIM), Cornell University, Ithaca, New York 14853, USA*

[d]*Center for Nanoscale Materials, Argonne National Laboratory, Lemont, Illinois 60439, USA*

[e] *Kavli Institute at Cornell for Nanoscale Science, Ithaca, New York 14853, USA*

Theoretical aspects

Partial and total phonon density of states were performed using the Phonopy framework [1] for VASP where ionic forces were computed following the fine displacement approach under the projector augmented-wave (PAW) [2,3] PBE functional [4,5]. The volume and shape of the unit cell were simultaneously optimized keeping ionic positions fixed using the experimental crystallographic information file (CIF) of the VO_2 M1 phase [6]. This optimization process largely reduces the normal unbalanced ionic forces encountered in experimental CIF files and avoids getting the VO_2 rutile phase as the ground state which is a normal outcome of the optimization under PBE [7]. Strain effect was simulated by linearly transforming the rutile lattice parameters of MgF_2 into the lattice basis of the VO_2 M1 phase using the following expression:

$$u^{TL} = M^{-1} N u^{Subs}$$

where *TL* is a top layer, u are the coordinates in the basis formed by the lattice vectors, M and N are the matrix representations of the lattice vectors of the *TL* and the substrate lattice correspondingly. Since this transformation preserves the vector direction and the orthogonality,

any changes by the strain can be added by a parameter directly to the norm of the vectors in this representation.

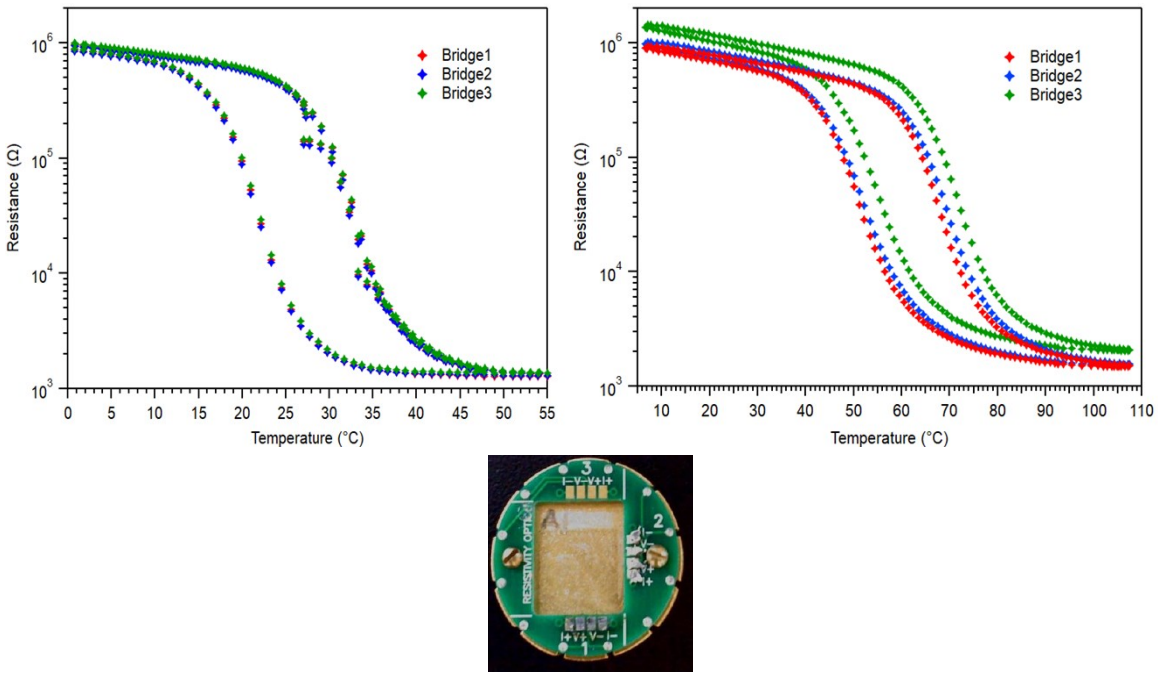

Figure S1. Temperature-induced electrical transport measurements of VO_2/MgF_2 (001) (top left) and (110) (top right) obtained via 4-points resistance measurement on 3 bridges at a time. The example of 3 bridges Resistivity puck is also depicted. The (001) VO_2 is completely isotropic, whereas (110) VO_2 film exhibits anisotropy.

Substrate	Lattice Parameters	Lattice Mismatch to VO_2
VO_2 (at 360K)	a_R = 4.5546 c_R = 2.8514	- -
(001) TiO_2	a_R = 4.5940 c_R = 2.9590	+0.9% -
(110) TiO_2	a_R = 4.5940 c_R = 2.9590	+0.9% +3.8%
(001) MgF_2	a_R = 4.6249 c_R = 3.0520	+1.5% -
(110) MgF_2	a_R = 4.6249 c_R = 3.0520	- +7.0%

Table S1. Lattice constants and rutile VO_2 lattice mismatch for different substrate orientations of TiO_2 and MgF_2. Lattice constants originate from literature; VO_2 at 87 °C [8], MgF_2 at 25 °C [9], TiO_2 at 25 °C. Lattice mismatch is predicted using the lattice parameters parallel to the substrate surface using the following equation: $a_{sub} - a_{film}/a_{film}$

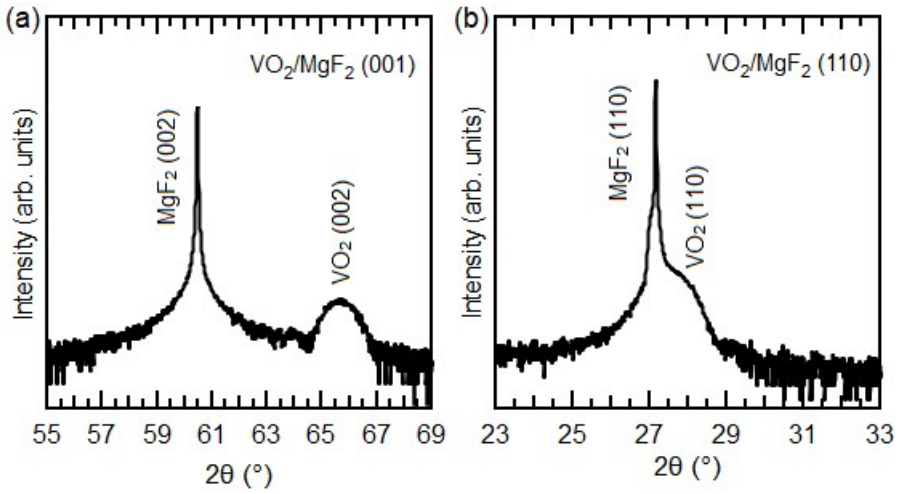

Figure S2. Room temperature XRD of 10 nm VO_2/MgF_2 (a) (001) and (b) (110)

The 10 nm VO_2/MgF_2 (001) and (110) films used in the Raman measurements both exhibited partial strain. Previously, VO_2/TiO_2 thin films have had high degrees of strain as TiO_2 is isostructural to VO_2 in its high temperature phase and has relatively low lattice mismatch [10]. MgF_2 is also isostructural to VO_2 however, as can be seen in Table S1, it has nearly the double lattice mismatch as to TiO_2. Based on the XRD (Fig. S2) the c-axis length of our VO_2/MgF_2 (001) film is 2.86 Å and VO_2/MgF_2 (110) film is 2.88 Å. Note that the (110) c-axis length was estimated assuming that the cell volume of VO_2 is the same as that of bulk (59.22×10^{-3} nm^3). Indeed, strain is achieved as the c-axis length of the (001) shrinks and the (110) elongates in relation to bulk c-axis length of 2.85 Å. Nevertheless, less strain was achieved in comparison to VO_2/TiO_2 thin films in both the (001) [10] and (110) [11] orientations due to exceptionally large mismatch with MgF_2 i.e. partially strained.

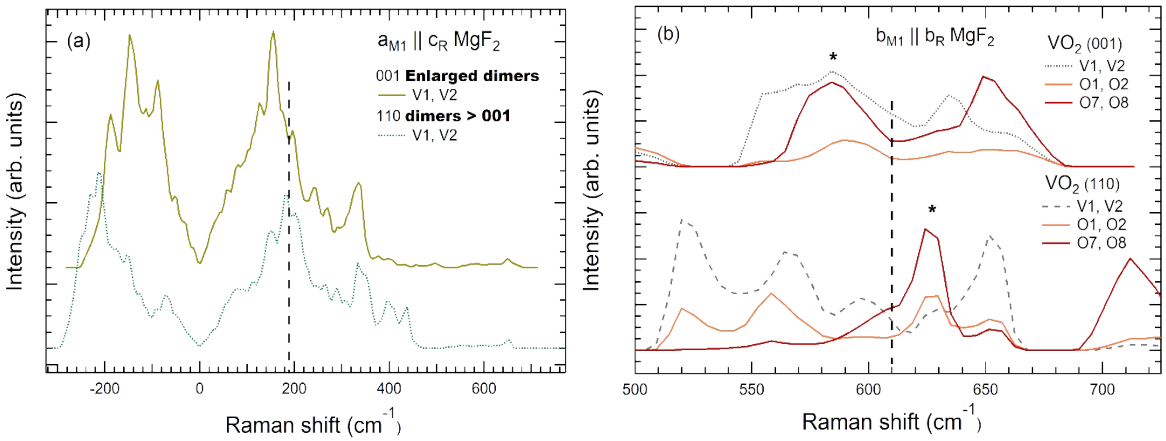

Figure S3. Partial phonon density of states along and perpendicular to the V-V dimer direction. The dotted line represents the bulk VO_2 [12,13]. The calculated red and blue shifts of the characteristic phonon modes reveal the strain effect on VO_2. The presence of the larger negative phonon mode range suggests the dynamical instability of VO_2 systems in the applied level of calculations. However, the applied theoretical approaches allow to capture strain-induced shift of the high frequency phonon modes (b).

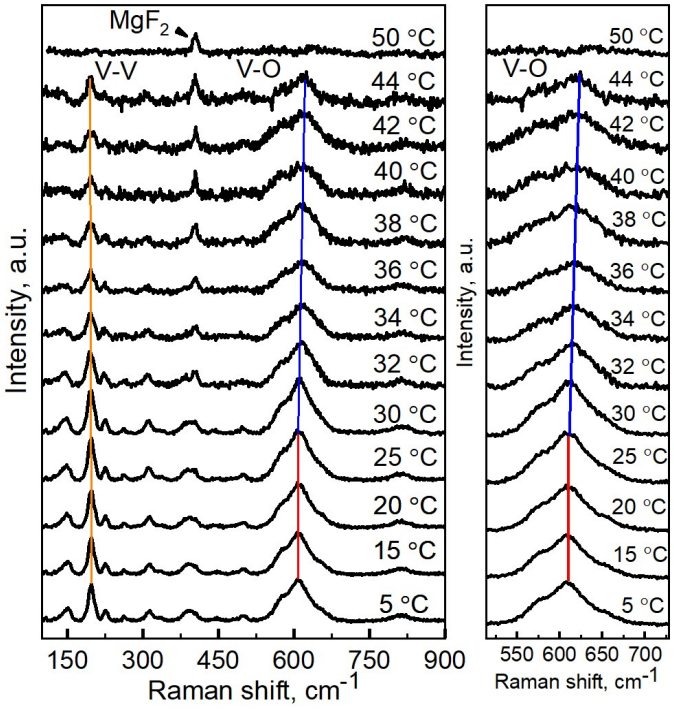

Figure S4. Raman spectra of VO_2/MgF_2 (001) at selected temperature points during cooling. The range around 600 cm-1 is additionally depicted. Color lines show the shift of characteristics Raman peaks.

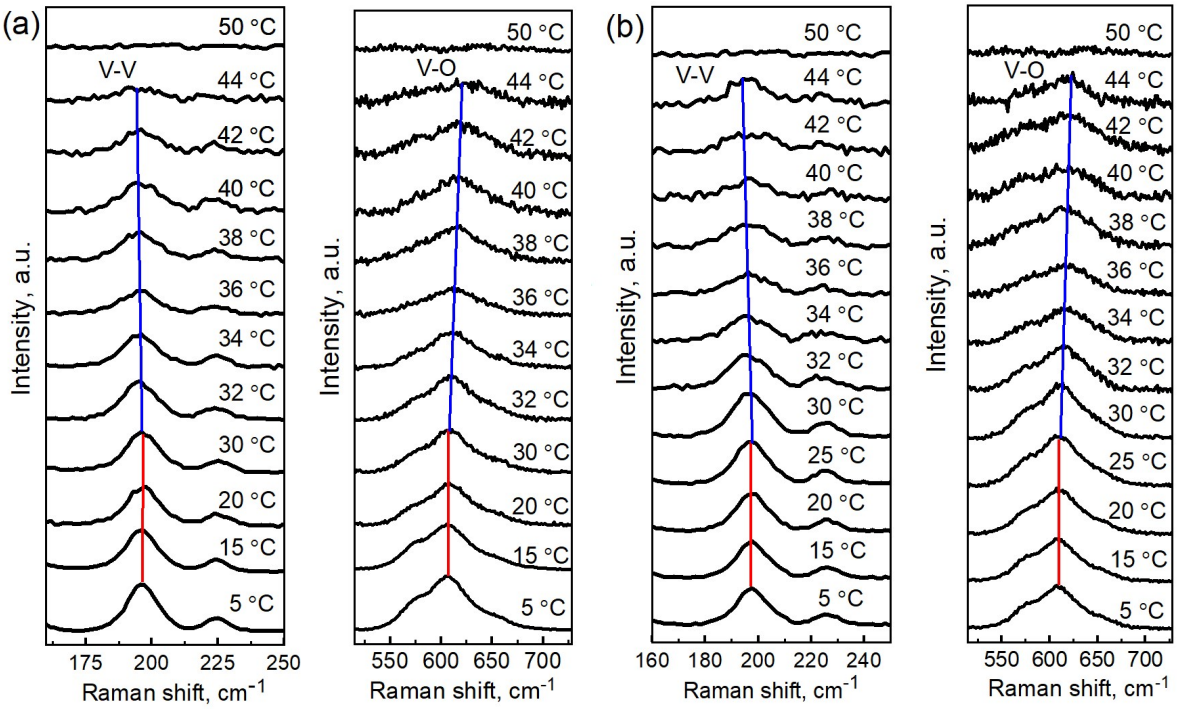

Figure S5. Evolution of characteristic VO_2/MgF_2 (001) Raman peaks during the heating (a) and cooling (b) steps.

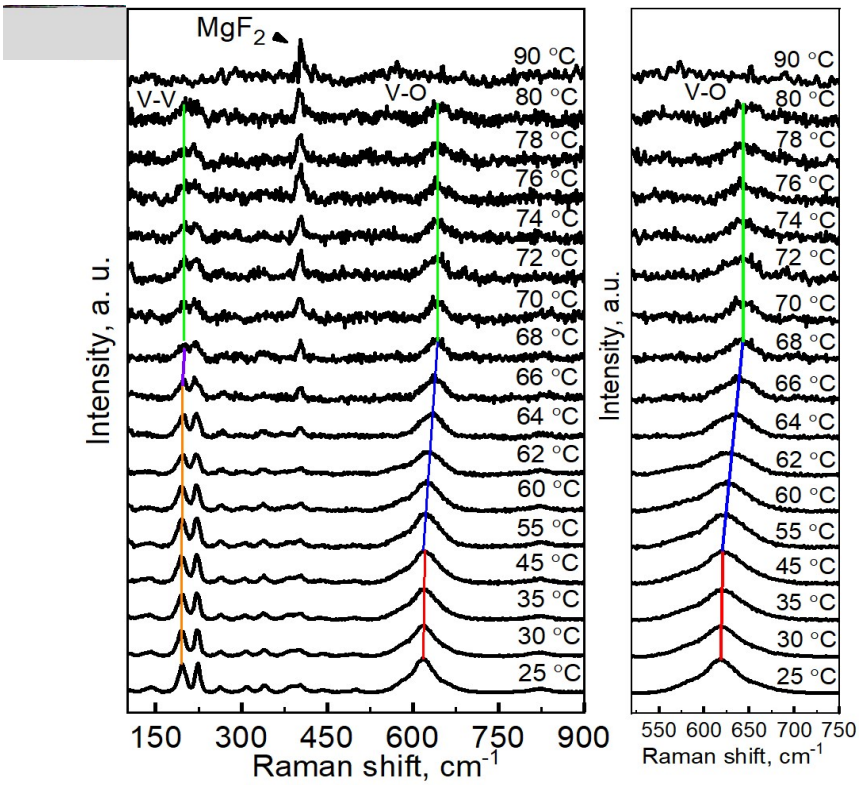

Figure S6. Raman spectra of VO_2/MgF_2 (001) at selected temperature points during cooling. The range around 600 cm^{-1} is additionally depicted. Color lines show the shift of characteristics Raman peaks.

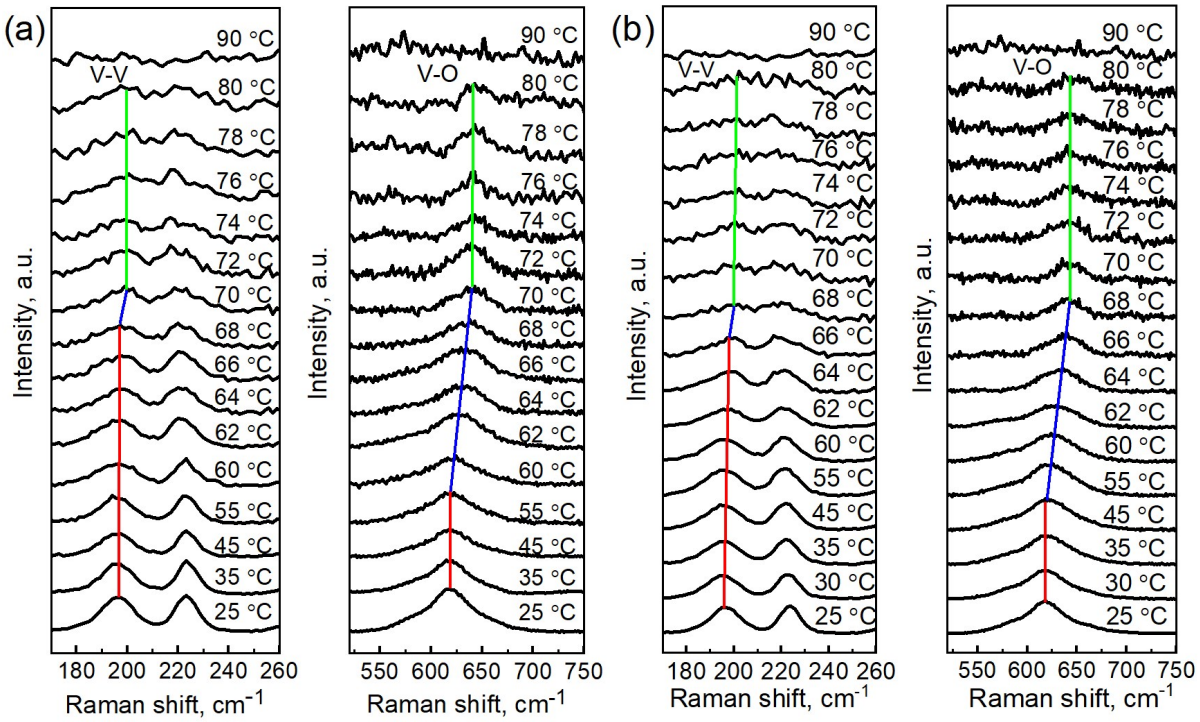

Figure S7. Evolution of characteristic VO_2/MgF_2 (110) Raman peaks during the heating (a) and cooling (b) steps.

References

[1] Atsushi Togo and Isao Tanaka, *Scr. Mater.*, 108, 1-5 (2015).

[2] P. E. Blöchl, *Phys. Rev. B* 50, 17953 (1994).

[3] G. Kresse and D. Joubert, *Phys. Rev. B* 59, 1758 (1990).

[4] John P. Perdew, Kieron Burke, and Matthias Ernzerhof, *Phys. Rev. Lett*. 77, 3865 (1997).

[5] John P. Perdew, Kieron Burke, and Matthias Ernzerhof, *Phys. Rev. Lett.* 78, 1396 (1997).

[6] G. Andersson, *Acta Chim. Scand.* 10, 623 (1956).

[7] Zhiyong Zhu and Udo Schwingenschlögl, *Phys. Rev. B* 86, 075149 (2012).

[8] D. B. McWhan, M. Marezio, J. P. Remeika, P. D. Dernier, *Phys. Rev. B* 10, 490 (1974)

[9] J. Haines, J. Légerm, F. Gorelli, D. D. Klug, J. S., Tse, Z. Q., Li, *Phys. Rev. B* 64, 134110 (2001).

[10] H. Paik, J. A. Moyer, T. Spila, J. W. Tashman, J. A. Mundy, E. Freeman, N. Shukla, J. M. Lapano, R. Engel-Herbert, W. Zander, J. Schubert, D. A. Muller, S, Datta, P. Schiffer, D. G. Schlom *Appl. Phys. Lett.* 107, 1-6 (2015).

[11] Y. Muraoka, Z. Hiroi, *Appl. Phys. Lett.* 80, 583-585 (2002).

[12] G. I. Petrov, V. V. Yakovlev, J. Squier, *Appl. Phys. Lett. 81*, 1023–1025 (2002).

[13] K. Shibuya, J. Tsutsumi, T. Hasegawa, A. Sawa, *Appl. Phys. Lett. 103*, 021604 (2013).